Design of the reflection magnet and its shielding effect analysis for the neutral beam injector of EAST

LIANG Lizhen* HU Chundong XIE Yuanlai WEI Jianglong XIE Yahong LI Jun

Institute of Plasma Physics, Chinese Academy of Sciences, Hefei 230031, China

Abstract In this paper, a reflection magnet to be installed in the EAST neutral beam injection system is simulated and designed. The field intensity of reflection magnet of 42-cm maximum bending radius is about 1.539×10^{-1} T for 100 keV deuterium beam. The shielding cage is formed by rods. Using the ANSOFT software, the magnetic shielding effect was estimated at about 3% at the magnet pole region.

Key words Neutral beam, Reflection magnet, Magnetic shielding, Shielding effectiveness

1 Introduction

Heating with neutral beam injection has been successful in various magnetic confinement devices[1,2]. As shown in Fig.1, a neutral beam injector for magnetic confinement device involves stages of powerful ion beam generation, ion beam neutralization, and separation and treatment of residual ions[3].

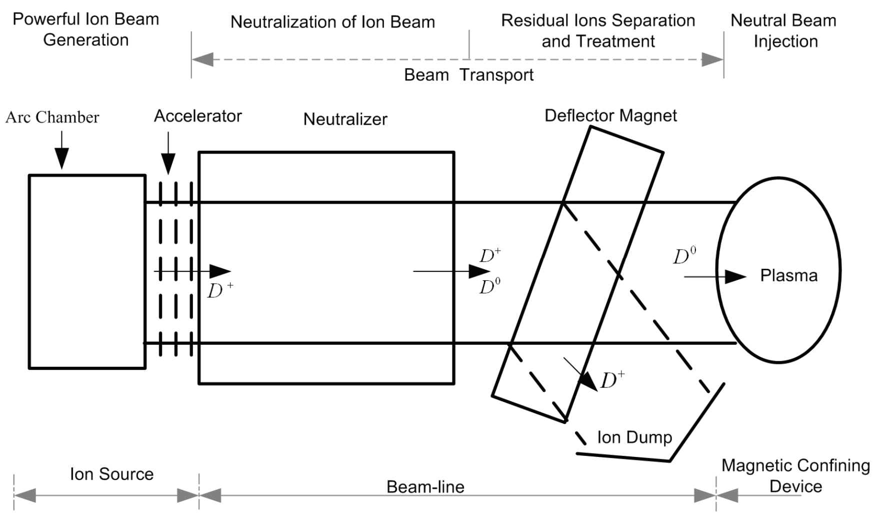

Fig.1 Block diagram of a neutral beam injector.

The neutral beam injection system of Experimental Advanced Superconducting Tokamak (EAST) consists of two injectors, each having vacuum vessel, neutralizer, reflection magnet, ion dump, calorimeter, and cryopump. Schematic of the neutral beam injection system is given in Fig.2. The vacuum vessel can be divided into three parts: Part 1: the rear cryopanel, neutralizer and ion dump; Part 2: the reflecting magnet; and Part 3: the front cryopanel and calorimeter[4,5]. The front cryopanel is of a circular disk with a large rectangular window at the center for the calorimeter, and the rear cylindrical cryopanel is coaxial with the beam-line vessel. A gas baffle is located between the neutralizer and reflection magnet, so as to optimize the vacuum distribution.

* Corresponding author. *E-mail address:* lzliang@ipp.ac.cn

Received: 2010-11-02

A separation magnet dumps the residual ions and produces a neutral beam. The residual ions may result in significant damage to the neutral beam injector by the thermal overload and by additional gas sources from ion desorption, wall outgassing and ion recombination. A parameter simulation for designing the reflection magnet had been performed. However, the neutral beam injector is immersed in stray magnetic field of the confining magnetic field coils[6], and the stray magnet is about 0.01 T at the separation magnet region. Therefore, the magnetic shielding in the residual ion separator region should to be reconsidered due to the cryopanel pumping speed and gas baffle.

Residual ions in the separation magnet deviate from the beam passage by the Lorentz force due to their circular motion in uniform magnetic field. Considering the device cost, the vacuum distribution in the injector and additional source of gas due to deposition of the residual ions, a 180º reflection magnet of vertical entry and exit was chosen for EAST neutral beam injector. Parameters of the magnetic field intensity, coil, magnet field region and protection louver were estimated. The intensity of reflection magnet field with the maximum bending radius of 42 cm is about 1.539×10^{-1} T for a deuterium beam at 100 keV.

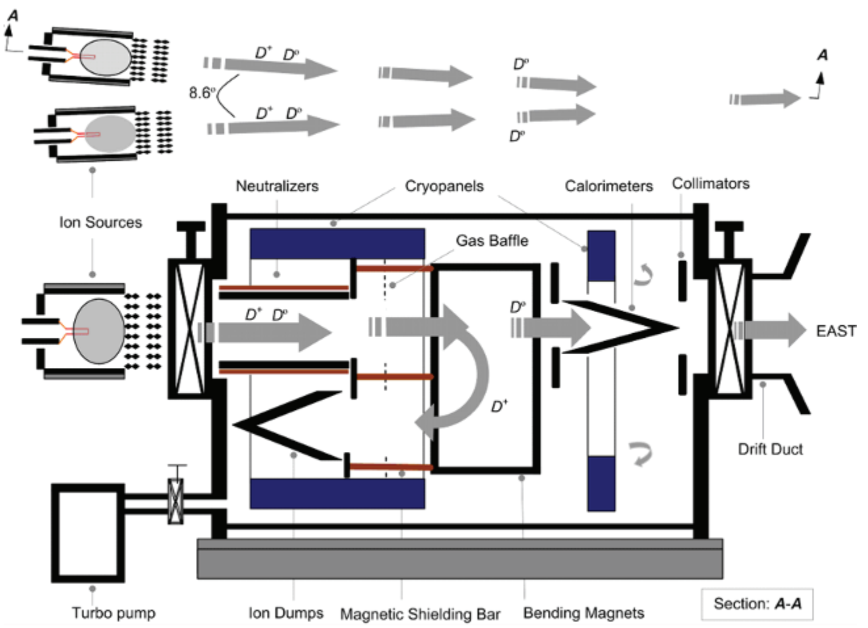

Fig. 2 Schematics of the neutrol beam injection system at EAST.

2 Parameter design of the reflection magnet

2.1 Magnetic field intensity design

Traversing a magnetic field, the Lorentz force is $F=qvB$, where q is the ion charge, v is the ion speed, and B is the magnetic field intensity. The radius of ion deflection is $R= mv/qB$, and the kinetic energy of ion in electrostatic extraction system is $E= qU =1/2mv^2$, where m is the ion mass, and U is the electrical potential difference.

Thus, the bending radius can be expressed by,

$$R=(2mE)^{1/2}/qB \quad (1)$$

Eq.(1) shows that for particles having the same charge/mass ratio, the deflection radius R is proportional to the square root of the ion energy in a certain magnetic field. The energetic beam from the neutralizer can be in three energy categories: full energy, half of the full energy and a third of the full energy. For a beam size of 12 cm×48 cm, in order to separate the residual ions from the beam passage and make full use of the space in the vacuum tank, the radius shall be no less than 24 cm for ions in 1/3 full energy. Fig.3 shows the process of the magnet reflection. When the ions in 1/3 full energy has the radius of 24 cm, the radii for the 1/2 energy and the full energy ions are 29.4 and 41.5 cm, respectively, hence the reflection radius of 42 cm for full energy ions.

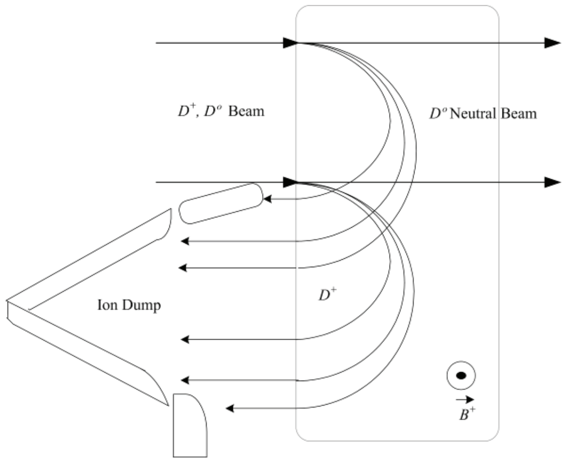

Fig. 3 The principle of the reflection magnet.

Fig.4 shows that the ion energy is 100 keV and magnetic field is 1.539×10^{-1} T at the 42-cm reflection radius for 100 keV ions. Considering a safety factor of 1.2, the 'H' type dipole magnet should provide 0.19 T uniform magnetic field.

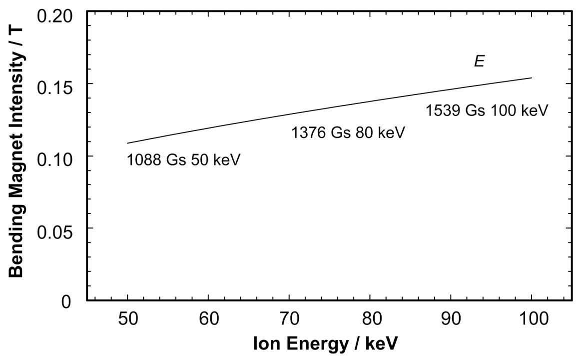

Fig.4 Relationship between magnetic field strength and deuterium ion energy.

2.2 Parameter design for coil

The excitation ampere turns can be calculated by

$$NI = \oint H dl = \oint_{L\text{air}} \frac{B}{\mu_0} dl + \oint_{L\text{iron}} \frac{B}{\mu} dl = \frac{B}{\mu_0} L_{\text{air}} + \frac{B}{\mu_0} L_{\text{iron}} [\frac{\mu_0}{\mu_{\text{iron}}}] \quad (2)$$

where, μ_0 is the vacuum permeability of the magnet coil, and μ_{iron} is the permeability of the magnet core and pole. The μ_{iron} is approximately constant and is larger than μ_0 for an unsaturated magnet core. So, Eq.(2) can be simplified into Eq.(3),

$$NI \approx L_{\text{air}}(B/\mu_0) \quad (3)$$

where, the magnetic field intensity is B ($\text{Wb}\cdot\text{m}^{-2}$), and L_{air} (m) is the pole distance for an 'H' type solenoid dipole. Considering divergence of the neutral beam, the reflection gap (g) should be no less than 20 cm, and the ampere- turn is about 33,500. Then the current densities for external/inner water cooling wires are about 3 and 10 $\text{A}\cdot\text{mm}^{-2}$ [7], and coil areas are 11,166 and 3350 mm^2, respectively. Because the magnet installation space is limited by the vacuum vessel, an inner cooling coil is a better choice, using 9.3 mm×9.3 mm square copper wire with a Φ6.5mm hollow. The coils include two-double subcoils with eight turns per gap, hence 64 turns for one beam passage gap.

2.3 Estimation for magnetic field region

At the 42-cm reflection radius (r_m), an available pole coefficient is calculated by

$$\xi = r_m/R' \quad (4)$$

where, ξ = 0.78–0.91 and R is radius of the magnet pole. For the 180º reflection magnet of vertical entry and exit, a rectangular section is employed for magnet pole. Considering the request of adjustable radius of ion deflection, the dimension for the magnet pole section is about 140 cm×50 cm.

2.4 Cooling water and magnet power supply

The coil maximum working current of about 472.5 A is delivered by the copper wire. Taking the magnet pole as inner dimension of the coil, the average wire length for every coil is 2×(140+50+4+4)×32=12672 cm. If the inner- cooled copper wire is at 25–40ºC, the coil resistance is $\rho L/s$=$(0.0203\times133.12)/\{0.0093^2-[(\pi/4)\times 0.0065^2]\}$ =0.0483 Ω.

In order to get a uniform magnetic field, magnet coils are used in the vacuum vessel for a series of power supplies at 45.6 V, and the heating power estimated by ohmic effect is about 10.8 kW. The total coil heat is taken out by the cooling water. The cooling water flow at a temperature rise of 25º is,

$$V = -P/(ct\rho) = 0.102 l/s \quad (5)$$

where, P is the coil heat power, t is the temperature rise, c is the heat capacity, and ρ is the cooling water density.

2.5 Protection louver design

During bending of the residual ions, a few ions are neutralized by collision with background molecules in the magnet gap, forming energetic atoms moving along the tangent direction of the bending track. The cryopanels are located behind the reflection magnet, with enough clearance to pump out the gas in the magnet gap. Consequently, the cryopanels are protected by a louver. Parameters of the particle tracks in magnet gap are shown in Fig.5, and the injection angles of the energetic atoms in the louver region can be calculated by Eqs.(6)–(9).

$$\theta_1 = \mathrm{ArcSin}(\frac{R}{\sqrt{w_p^2+(w-R+r)^2}}) + \mathrm{ArcTan}(\frac{w-R+r}{w_p}) \tag{6}$$

$$\theta_2 = \mathrm{ArcSin}(\frac{R}{\sqrt{w_p^2+(w-R+2R)^2}}) + \mathrm{ArcTan}(\frac{w-R+2R}{w_p}) \tag{7}$$

$$\theta_3 = \mathrm{ArcSin}(\frac{R}{\sqrt{w_p^2+(R-r)^2}}) - \mathrm{ArcTan}(\frac{R-r}{w_p}) \tag{8}$$

$$\theta_4 = \mathrm{ArcSin}(\frac{R}{\sqrt{w_p^2+(R)^2}}) + \mathrm{ArcTan}(\frac{R}{w_p}) \tag{9}$$

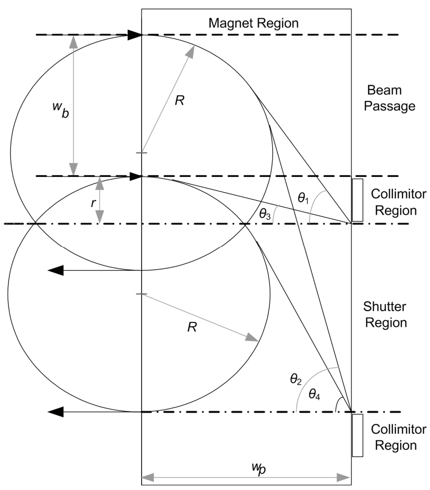

Fig. 5 Track for particle in magnet gap.

The critical angle for louver protection is defined by Eq.(10), and its parameters are shown in Fig.6(a).

$$\beta = \mathrm{ArcTans}(s/l\cos\alpha) \tag{10}$$

With R= 42 cm, w_p=64 cm, r=18 cm and w_b=48 cm, the magnet louver of the neutral beam injector is shown in Fig.6(b). Thus energetic atoms from the neutralization in bending magnet gap cannot collide with the cryopanels.

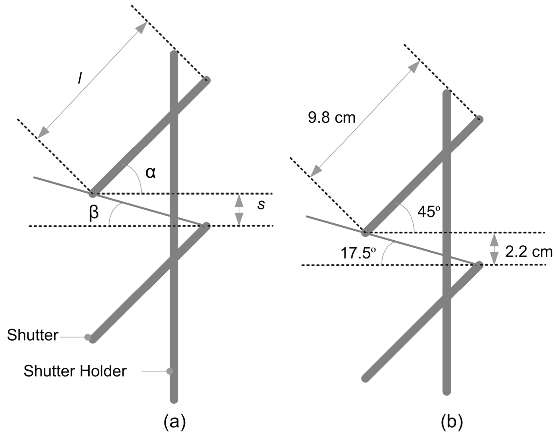

Fig.6 Principle for louver protection.

3 The analysis of magnetic shielding

3.1 Magnetic shielding requirements

Energetic particles are sensitive to magnetic fields. The strong magnetic field can reduce beam transmission efficiency, and the beam power loss may damage the inner elements, so the typical field strength is less than 5×10^{-4} T in the region of magnet pole along the beam passage. Also, the pumping speed should be designed in the magnetic shielding. As the rear cylindrical cryopanel is coaxial with the beam-line vessel, the magnetic shielding should leave enough clearance for cryopump.

3.2 Magnetic shielding principle and design

Magnetic shielding is not really ‘shielding’ in common sense. Magnetic field lines, which are in continuous loops from the north pole to the south pole, cannot be stopped or blocked. The key to magnetic shielding is to redirect magnetic fluxes so that they do not enter an area of interest. Usually, there are two ways to do this: to provide magnetic fluxes with good pathways and to use repulsive force acting on the magnetic flux with a reverse magnetic field being added to the area of interest. The first method is widely used due to its lower cost and convenience. For the EAST neutral beam injector, we will use this method to protect ions from the stray magnetic field of tokamak. It is serves with two basic actions: preventing strong field radiation from sources, and shielding the ion beams from external magnetic fields.

Figure 7 shows that when a magnetic line passes through the interface between two magnetic media, it is refracted according to the refraction law of $\tan\theta_1/\tan\theta_2 = \mu_1/\mu_2$. When the incidence line goes in a larger θ_1, the magnetic line is refracted farther. And the permeability of magnetic shielding material is larger than that of vacuum. Therefore, the best shielding effect can be achieved with the shield surface being parallel or nearly parallel to the magnetic field lines.

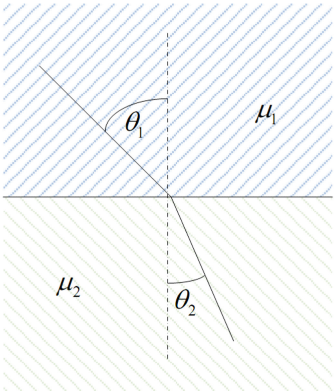

Fig.7 Magnetic line transmission at the medium boundary.

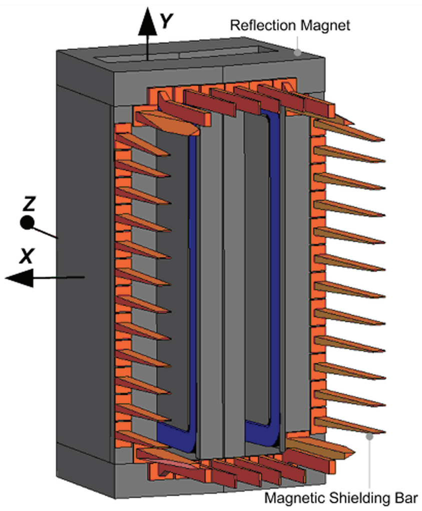

Fig.8 Arrangement of the magnetic shielding bar.

To maximize the flow of cooling gas from the region occupied by the neutral and reflected ion beam to surrounding cylindrical cryopanel, we use the shielding cage formed by the rod material with a declining surface as the magnetic shielding bar. Taking into account the stray magnetic field mainly along the axis of the tokamak, the cost of magnetic shielding and the machining convenience, a wedge-shaped magnetic shielding rod in Fig.8 is employed.

At the pressure of about 10^{-2} Pa in the separation region of residual ions, the mean free path of collision between gas molecules is about 1 m. The background molecules collide with the component surface, hence a molecular flow. On the other hand, at a uniform temperature distribution, the conductance for a rectangular duct is

$$C=(309ka^2b^2)/[L_{duct}(a+b)] \tag{11}$$

where, a, b and L_{duct} are side lengths and the duct length, respectively; and k is a function of a to b, with $k(1)=1.1$, $k(0.5)=1.15$, $k(0.33)=1.20$, $k(0.2)=1.30$, and $k(0.1)=1.44$.

This magnetic shielding has a conductance in parallel. Thus, the duct length is the thickness of the magnetic shielding bar. It is very small, thus, the conductance of the magnetic shielding is enough for cryopanel pumping. By simulating the magnetic shielding fingers, the optimal bar number is 40, to form a suited conductance and shielding efficiency.

4 Results

4.1 Simulation of magnetic field

Modeling of reflection magnet, including the coils, yoke and shielding bars, was carried out. The coil currents were assigned with 250, 300, 350, 400, 450 and 500 A, respectively, for the magnet intensities of 0.0977, 0.1174, 0.1375, 0.1565, 0.1765 and 0.1957 T on the middle plane in the gap. The excitation coefficient is about 1.02. In order to obtain reflection magnetic field in Fig.4, a current of 277–392 A is required for a 50–100 keV beam operation. The magnetic field distribution on the middle plane in the gap is shown in Fig. 9, at the coil current of 450 A. It shows a uniform magnetic field at the pole region.

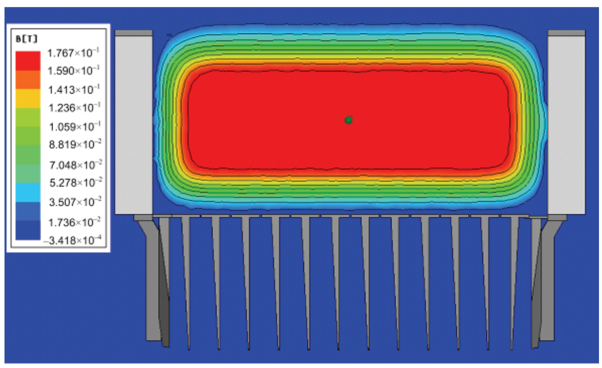

Fig.9 Magnetic field distribution on the middle plane in the gap.

4.2 Simulation results of magnetic shielding

In order to verify the effect of magnetic shielding, three models were designed by ANSOFT software (Fig.10), with two permanent magnets on the upper and lower ends of the reflection magnet. With and without the magnetic shielding bar and reflection magnet, the magnetic shielding effect was estimated by comparing the magnetic field intensity in the magnetic shielding region, and analyzed by the three models. Model 1 has 20 magnetic shielding bars installed symmetrically at the magnet upstream. Model 2 has 40 magnetic shielding bars. Considering the installation of the gas baffle, Model 3 has two magnetic shielding arrays, each consisting of 40 magnetic shielding bars in structure the same as that in Model 2.

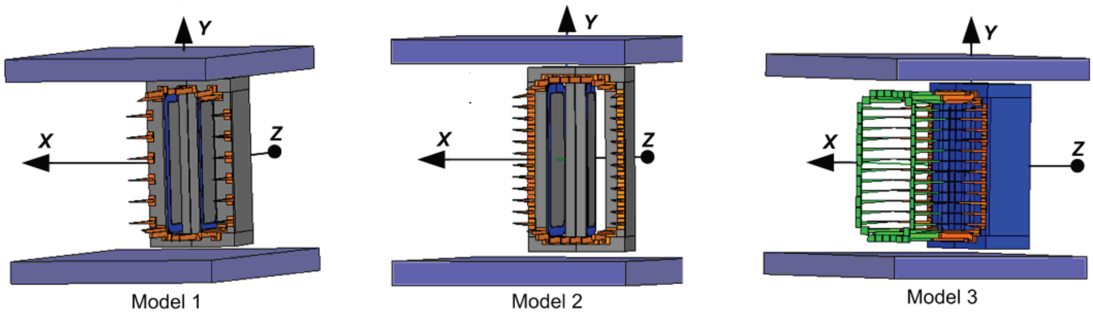

Fig.10 Models for magnetic shielding analysis.

Fig. 11 shows the shielding effect at the gap center line along ***Z*** direction. The farther the distance away from the end of the magnetic shielding bar, the better the magnetic shielding effectiveness is. It can be balanced up to about 3% by the three models in the magnet pole region. Comparing Model 1 with Model 2, the more magnetic shielding bars, the better magnetic shielding effect is. Comparing Model 2 with Model 3, the magnetic shielding effect improves with longer shielding bars due to space effect, but no clear primary shielding. Considering the vacuum pump, magnet maintenance and installation space, Model 3 is used for the EAST neutral beam injector, and the gas baffle is installed between two magnetic shielding bars.

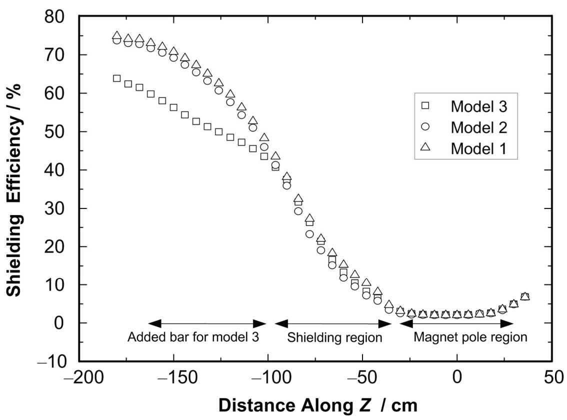

Fig.11 Shielding effectiveness along the ***X*** axis at the center of magnetic pole gap.

5 Conclusions

The reflection magnet for the EAST neutral beam injector was physically designed. With a bending radius of 42 cm, the field strength is about 1.539×10^{-4} T for 100 keV deuterium beam. A uniform magnetic field is obtained using a dipole magnet. The square copper conductor of 9.3 mm×9.3mm with a Φ6.5mm hollow is chosen for the coils. The neutral ion beam injector works at the continuous wave, so a 0.107 L/s cooling water is needed. A protection louver is used for keeping the neutralized energetic particles from colliding with the cryopanels. With two magnetic shielding bar arrays, the magnetic shielding effect in the magnet pole region is about 3%.

Acknowledgements

This work is supported by the Knowledge Innovation Program of the Chinese Academy of Sciences: the study and simulation on beam interaction with background particles in neutralization area for NBI, and the key technical and physical problems study for neutral beam steady-state operation. It is also supported by National Natural Science Foundation of China under Grant No. 10875146.

References

1 Wesson J. Tokamaks. Oxford: Oxford Clarendon Press. 1997, 243–257.

2 Gibson G, Lamb W, Lauer E. Physical Review, 1959, **14:** 937–942.

3 Speth E. Rep Prog Phys, 1989, **52:** 57–112.

4 EAST neutral beam injector physical design (Internal Report).

5 Colleraine A P, Doll D W, Holland M M, *et al.* 780953-5: a parametric study of the Doublet III neutral beam injection system. 10 symposium on fusion technology, Padova, Sep 1978, 207–215.

6 Dewitt R, Low W. 790012-133: The DIII neutral beam shieding. 8 Symposium on Engineering Problems of Fusion Research. San Francisco, Calif, Nov 1979, 1844–1848.

7 Li Z, Zhao W. Electric Handbook. Abhui: Anhui Science and Technology Publishing House, 2002, 1559–1625.